J Mater Sci: Mater Electron (2017) 28:15694–15700
DOI 10.1007/s10854-017-7459-4

A thermally conductive epoxy polymer composites with hybrid fillers of copper nanowires and reduced graphene oxide

Manni Li[1] · Cheng Tang[1] · Li Zhang[1] · Beirong Shang[1] · Shuirong Zheng[1] · Shuhua Qi[1]

Received: 9 June 2017 / Accepted: 1 July 2017 / Published online: 8 July 2017

Abstract A thermally conductive epoxy polymer composite comprising copper nanowires and reduced graphene oxide as hybrid fillers was prepared. The synthesized one-dimensional copper nanowires (CuNWs) with excellent thermal conductivity and easy dispersity performed a thermal bridge to connect different layers of dimensional graphene oxide (GO), which benefited the thermal conductivity of epoxy composite conductor with increasing hybrid filler loading. The microstructure and morphology of hybrid fillers as well as the thermal properties, volume resistivity and dielectric constant of epoxy polymer composite were investigated. The TEM of hybrid fillers confirmed that CuNWs were loaded on the NH_2-rGO uniformly and the CuNWs/NH_2-rGO/epoxy possessed higher thermal conductivity and lower volume resistivity (the thermal conductivity and volume resistivity were about 0.43 W/(m·K) and 2.69×10^{11} Ω·cm, respectively) compared to CuNWs/epoxy polymer composite and NH_2-rGO/epoxy polymer composite. Moreover, the CuNWs/NH_2-rGO/epoxy composites presented better dielectric constant. These were all contributed to the synergetic effect between CuNWs and rGO.

1 Introduction

Miniaturization of electronic devices and integrated circuits results in the increase of heat generated in high density electronics. In order to ensure the good performance and long life of electronic devices, the heat dissipation of material becomes more and more important [1–4]. The thermal conductivity of composite is a vital material property in many application areas [5–12]. Because of its light weight, good electrical insulation and easy processing, polymer is often used as packaging materials for electronic circuits. However, due to the low thermal conductivity of the polymer itself, it is often necessary to add fillers with high thermal conductivity to the polymer to improve the thermal conductivity of the composite. There are various thermal conductive fillers, including AlN [13, 14], Al_2O_3 [15], BN [16], Ag [17], SiC [18] and so on, have been used to improve the thermal conductivity of polymer matrix. However, a large amount of fillers are indispensable to meet the requirement of thermal conductivity, which would deteriorate the viscosity, processing and other properties of epoxy.

Lately, metallic nano-materials have become a hot and new topic in materials science [12, 19–21]. Synthesize a new one-dimensional metallic nanomaterials with green approaches and low cost has caused widely concern. CuNWs, a kind of ideal one-dimensional copper nanostructures, was frequently used as the modified materials of polymer. Copper nanowires possess not only similar properties of good thermal conductivity, electrical conductivity, and ductility to Ag and Au nanostructures but also the cheap price, abundant reserves and other advantages [22]. Hence, copper has gradually become the best choice to replace Ag and Au nanomaterials and has great potential to fabricate high thermal conductive polymer composites.

Up to now, graphene has always been a topic of researchers owing to its excellent properties, such as superior mechanical property [23], high flexibility [24], and good optical, thermal, electrical properties [25–27]. Therefore, graphene can be naturally used as thermal conductive filler

✉ Shuhua Qi
qishuhuanwpu@163.com

[1] Key Laboratory of Polymer Science and Technology, School of Science, Northwestern Polytechnical University, Xi'an 710129, China

to improve the thermal conductivity of composites. Goyal et al. [28] prepared electrically conductive thermal interface materials with the hybrid graphene-metal particle fillers and showed that the thermal conductivity of resulting composites was increased by 500% at a small graphene loading fraction of 5 vol%. Wu et al. [29] prepared graphene nanoplatelet paper and found that the thermal conductivity of self-standing flexible paper can reach to 313 W $(mK)^{-1}$. Fang et al. [30] prepared eicosane-based phase change materials and showed that the thermal conductivity of eicosane was dramaticlly increased in the presence of graphene. Consequently, we choose reduced graphene oxide with active amino groups as thermal conductive fillers to improve the thermal conductivity of composite.

The idea of applying a hybrid filler consisting of two or more filler materials has already been discussed in paper and it has been testified that the improvement of composite properties can be acquired by combining the advantages of each filler [31, 32]. Considering the high thermal conductivity of graphene and copper nanowires, we combined CuNWs with rGO as hybrid filler to prepare high thermal conductive composite to maximize the thermal conductivity. In this paper, first, copper nanowires have been successfully synthesized and they possessed high aspect ratio, uniform diameter, good dispersity and morphology. Then another kind of reduced graphene oxide filler was also prepared. Subsequently, we used the two kinds of conductive fillers to synthesize thermal conductive epoxy polymer composites and investigated the thermal conductivity of composites. The result indicated that the CuNWs/NH_2-rGO/epoxy composites exhibited higher thermal conductivity compared with epoxy resin and epoxy composites prepared with each filler alone.

2 Experimental

2.1 Materials

Glucose anhydrose and copper chloride ($CuCl_2.2H_2O$) were obtained from Shanghai Han Si Chemical Co. Ltd. oleic acid and oleylamine were purchased from MACKLIN. Polyvinylpyrrolidone (PVP) was purchased from Aladdin Chemistry Co., Ltd. The graphene oxide (GO) nanosheets were produced from natural graphite flakes by the modified Hummers method [33], γ-aminopropyltriethoxysilane (APTES) was purchased from Jingzhou Jianghan Fine Chemical Co. Ltd (Hubei, China). Epoxy was purchased from Tianjin Kailida Chemical Trading Co., Ltd. (Tianjin, China), m-Xylylenediamine (MXDA) were purchased from Sinopharm Chemical Reagent Co., Ltd. (SCRC, China). Ethanol and hydrazine hydrate were purchased from Tianli Chemical Reagents Co. Ltd (Tianjin, China). All reagents were of analytical grade and used as received without further purification.

2.2 Preparation of NH_2-rGO hybrid

Nano-composite of NH_2-rGO was obtained by two steps: (1) the reaction of APTES with GO, and (2) reducing the products of step one with hydrazine hydrate to achieve NH_2-rGO.

The reaction of step one was realized as follows: 0.30 g GO, 10 mL deionized water and 190 mL ethanol were added into a beaker and treated under ultrasonication for 30 min. Subsequently, the mixed solution was transferred to a 250 mL three-necked flask with mechanical stirrer, reflux-condenser and constant-pressure funnel. Then, the mixture of 2 mL APTES and 30 mL ethanol was added to the flask dropwise. After that, the mixture was heated to 78 °C and kept for 4 h. The synthesis route was shown in Fig. 1. After the reaction completed, the resulting product was washed with ethanol for several times and coded as NH_2-GO. Finally, the prepared NH_2-GO was dried in vacuum oven at 60 °C overnight.

The second step as follows: the synthetized NH_2-GO was dispersed in 180 mL deionized water under ultrasonication for 30 min. The mixed solution was transferred to a 250 mL three-necked flask with reflux-condenser and mechanical stirrer, followed by 2.5 mL hydrazine hydrate and 7.5 mL ammonia. When the reaction temperature was up to 98 °C and kept for 6 h. After the reaction completed, the resulting product, recorded as NH_2-rGO, was washed with deionized water and ethanol for several times, and dried in vacuum oven at 60 °C overnight.

2.3 Preparation of CuNWs

Copper nanowires were successful synthesized by liquid phase reduction method [34]. First, 0.1220 g copper chloride ($CuCl_2.2H_2O$), 0.0875 g dispersion agent polyvinylpyrrolidone (PVP), 0.1420 g reducing agent glucose and 14.0 mL deionized water were added into a 50 mL beaker under magnetic stirring and marked as solution I Second, 1.4 mL oleylamine (OM) and 14 μL oleic acid (OA) dual ligands used as the stabilizing agent, 2.5 mL ethanol solution were added into a 100 mL three-necked flask under magnetic stirring and marked as solution II Then solution I was added into solution II and diluted with deionized water to 72 mL followed by 50 °C oil bath and magnetic stirring for 12 h. The color of the mixed solution changed from blue to caesiou. Subsequently, the mixture was transferred to a Teflon-lined autoclave and reacted at 116 °C for 6 h. The resulting solution was quickly washed with deionized water and ethanol three or four times and centrifuged at 2000 rpm for 10 min. At last, the reddish brown CuNWs

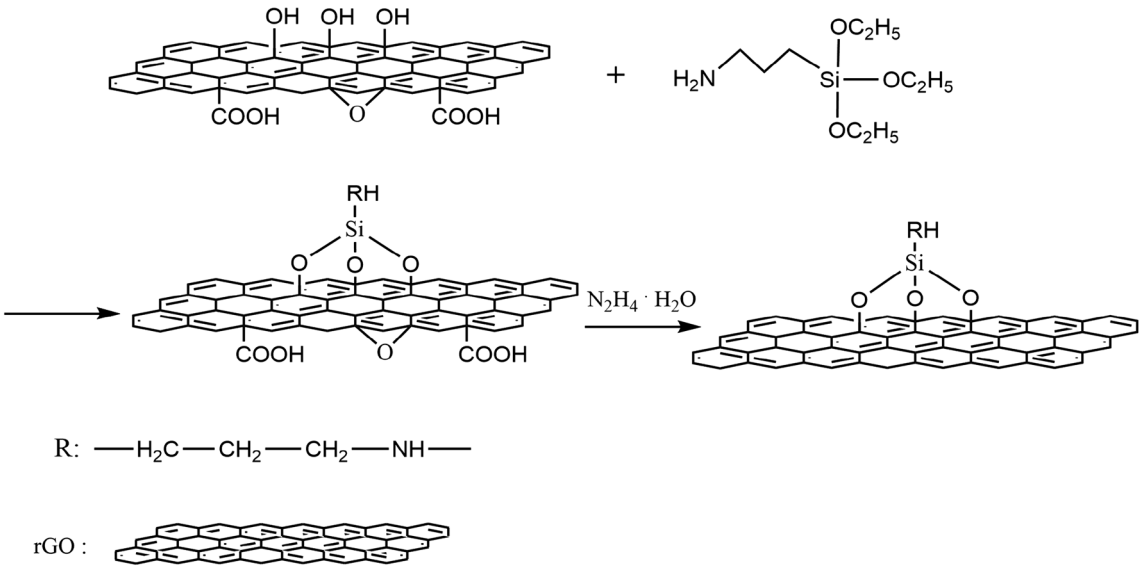

Fig. 1 The synthesis route of APTES coated rGO

were obtained and conserved in ethanol solution to form CuNWs suspension for use.

2.4 Preparation of epoxy composites

First, the prepared CuNWs, NH_2-rGO and hybrid filler CuNWs/NH_2-rGO were dispersed in ethanol for 30 min by a high amplitude ultrasonicator to disperse uniformly. Then, the fillers were incorporated into epoxy resin in different proportions and processed for 30 min continuously at the temperature of 60 °C to evaporate part of solvent. Afterwards, the proper curing agent m-Xylylenediamine (MXDA) was added into epoxy resin under ultrasonication and stirring. When the epoxy resin and curing agent dispersed uniformly, the mixture was poured into preheated mold and degassed in vacuum oven to remove bubbles. Ultimately, the mixture was cured steeply at 60 °C for 12 h, 80 °C for 6 h, 120 °C for 5 h. The interaction between CuNWs and NH_2-rGO was illustrated in Fig. 2 .

2.5 Characterization

Fourier Transform Infrared (FT-IR) spectra experiments of GO and NH_2-rGO were executed between 400 and 4000 cm^{-1} using a PberkinElmer-283B FT-IR Spectrometer. The samples were blended with potassium bromide (KBr) powder by grinder, and then pressed into flake to test.

X-ray diffraction (XRD) investigation was recorded on a X'Pert Pro MPD diffractometer with Cu Kα radiation

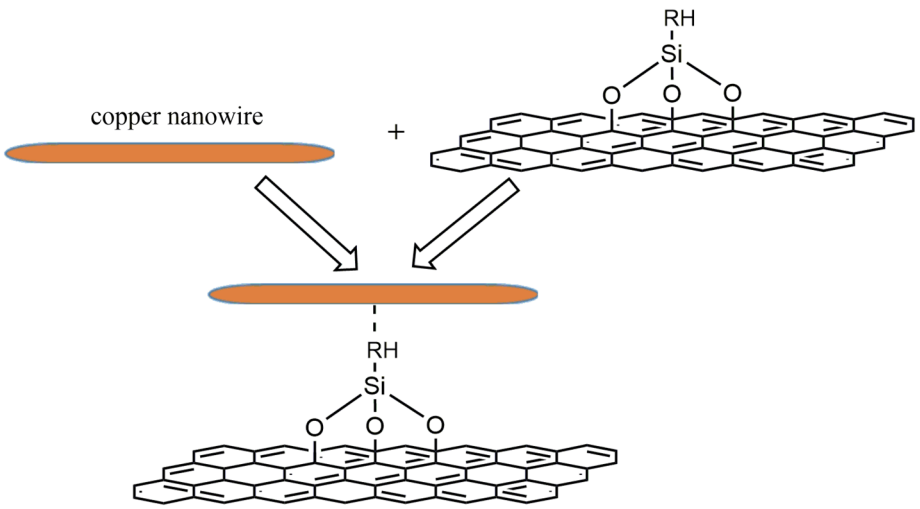

Fig. 2 The interaction between CuNWs and NH_2-rGO

(λ = 0.154178 nm). The current was 20 mA, and the tube voltage was 36 kV. Scans were taken over the 2θ range from 5° to 85° with the scanning rate of 0.02° s^{-1}.

The scanning electron micrographs (SEM) of the sample morphology was observed on a HITACHIS-570 instrument. The samples were glued to the conductive adhesive and sputtered with a thin layer (about 10 nm) of gold, and then to test.

High resolution transmission electron microscopy (HRTEM) images were obtained with a JEOL JEM-200CX microscope operating at 200 kV.

The thermal conductivity of composites are measured using a Hot Disk instrument (AB Corporation, Sweden) by standard method, which is based upon a transient technique. The measurements are performed on two-side parallel samples (specimen dimension for 10 mm × 10 mm × 3 mm) by putting the sensor (3.2 mm diameter) between two slab shape samples. The sensor supplies a heat pulse of 0.03 W for 20 s to the samples and the associated change in temperature is recorded. Finally, the thermal conductivity of the individual samples is achieved.

Volume electrical resistivity were performed by a ZC36 high impedance meter (Shanghai Precision Scientific Instrument Co., Ltd, China).

The thermal gravimetric analysis (TGA) tests were obtained by using a Perkin Elmer TGA-7 (USA) at a heating rate of 10 °C min^{-1} in a nitrogen atmosphere from 50 to 800 °C.

The dielectric constant of composites were tested by a high frequency QBG-3 Gauger over a wide frequency from 10 MHz to 60 MHz.

3 Results and discussion

3.1 Characterization

In order to confirm the reduced grapheme oxide modified by KH550 was successfully obtained, FT-IR spectra of GO and NH_2-rGO were conducted and showed in Fig. 3. The main characteristic peaks of GO at around 3394, 1708 and 1070 cm^{-1} correspond to –OH, C=O and C–O vibration, respectively. Then, the absorption peaks of NH_2-rGO/CuNWs emerged at around 3442, 1402 and 1114 cm^{-1}, respectively, which were assigned to –NH, –CN and –Si–O–C. Compared with the spectra of GO, the absorption peaks of –OH stretching vibrations almost disappeared in the spectra of NH_2-rGO. It may be attributed to two reasons. First, the –OH has been reduced by N_2H_4. Second, plenty of –OH have been reacted with APTES. Similarly, because of reduction, C=O and C–O became much weaker than that in GO, which proved GO has been reduced. Furthermore, the emergence of new absorption peaks of –NH, –CN and –Si–O–C indicated that GO has reacted with APTES. All of the evidence showed that the NH_2-rGO has been prepared successfully.

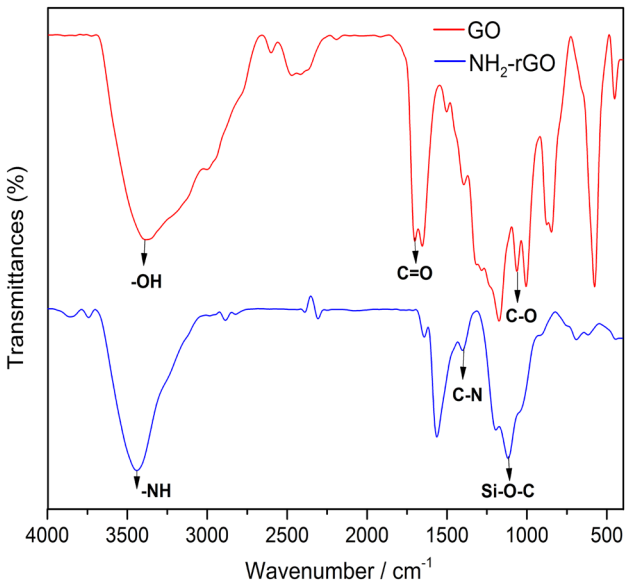

Fig. 3 FT-IR spectra of as-prepared GO and NH_2-rGO

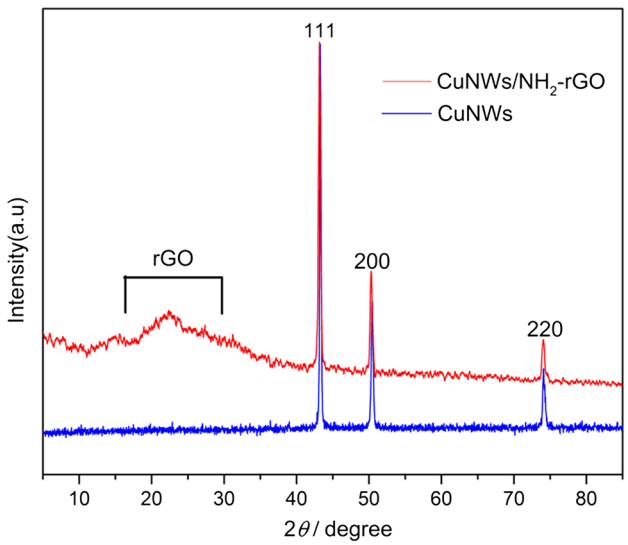

Fig. 4 XRD curves of CuNWs and CuNWs/NH_2-rGO

The structural characterization of as-prepared CuNWs and NH_2-rGO/CuNWs were investigated using X-ray diffraction (XRD) and shown in Fig. 4. In the XRD of CuNWs, there were three obvious diffraction peaks at 2θ = 43.31°(111), 50.48°(200), 74.18°(220) (JCPDS File No. 04-0836) corresponded to the face-centered cubic (fcc) of Cu of CuNWs. In addition, there were no other impurity peaks such as CuO and Cu_2O to be found, manifesting that the prepared CuNWs were of high purity. The strength

of the peak was the largest at $2\theta = 43.31°$, confirming the [111] was the preferential growth direction of CuNWs. In the In the XRD patterns of CuNWs/NH_2-rGO, we can find new peak of NH_2-rGO at $2\theta \approx 23°$ was produced, indicating the CuNWs/NH_2-rGO were successfully prepared.

The microstructure of prepared CuNWs using dual ligands OM and OA as stabilizing agent, PVP as dispersion agent for 6 h was analyzed by the SEM, as shown in Fig. 5a. From the curve, we can analyze that the prepared CuNWs had a length of 80 ± 15 μm, a diameter of 45 ± 5 nm. It was clear that the prepared copper nanowires had high aspect ratio, uniform diameter, good dispersity and morphology. In the growth process of CuNWs, OM and OA coated copper ion and formed a small droplet (equivalent to seed). With the increase of temperature, these seeds gradually grew into copper nanoparticles and further became the final nanowires. PVP acted as dispersion agent and surfactant as well as structure reducing agent in the growth process of CuNWs, so resulting CuNWs can be well dispersed in polar solvents. Figure 5b was the HRTEM image of NH_2-rGO, showing that the NH_2-rGO had clear, smooth surface and the sheet-like morphology with 1–2 layers. Figure 5c was the representative CuNWs/NH_2-rGO. It was clear that CuNWs were loaded on the NH_2-rGO uniformly and indicated that NH_2-rGO nanosheets and CuNWs were well compounded. Figure 5d was the cross-sectional SEM image of the CuNWs/NH_2-rGO epoxy composite. As shown, the hybrid fillers of NH_2-rGO and CuNWs can well dispersed in the epoxy matrix. This may be because the amount of the hybrid fillers was little and modified reduced graphene oxide can well combined with epoxy.

In order to illuminate the thermal properties of composite, Fig. 6 showed the thermal conductivity of composites. With the increasing of fillers loading from 0 to 0.8 wt%, the thermal conductivity increased gradually. In particularly, the thermal conductivity of CuNWs/NH_2-rGO/epoxy was higher than that of the same loading amount of NH_2-rGO/epoxy and CuNWs/epoxy composite, proving that the two kinds of fillers had synergistic effect when using together. First, interfacial adhesion [35, 36] between CuNWs and active amino groups on reduced graphene oxide allowed CuNWs to perform a thermal bridge to connect different layers of dimensional graphene oxide, which promoted the formation of perfect thermal conductive network and led to the high thermal conductivity of the composites. Besides, modified graphene can improve the interfacial interaction between fillers and the epoxy matrix. When the interfacial interaction between the fillers and resin matrix enhanced, the interfacial thermal conductivity also gets improved significantly [37].

The volume resistivity curve of pure epoxy and its composites were shown in Fig. 7. As expected, compared with the pure epoxy, the volume conductivity of composites were lower. It indicated that the conductive network of fillers in resin matrix have formed. According to the mechanisms of electrical conduction, there was a percolation density of the fillers in the insulating matrix and the fillers can contact with each other and perfect network will be formed when above the percolation density. Therefore, the electrical conductivity of the composites will improve. The synergetic effect of CuNWs and NH_2-rGO can make CuNWs contact each other and form perfect conductive networks,

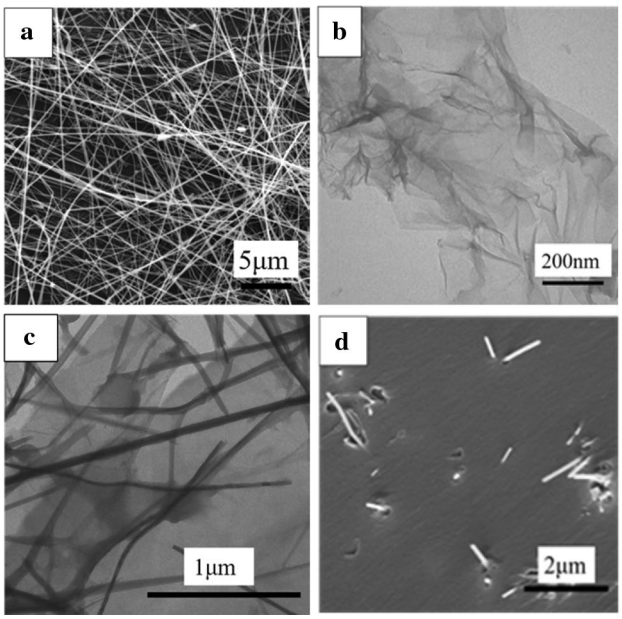

Fig. 5 **a** SEM image of as-prepared CuNWs; **b** TEM image of NH_2-rGO; **c** TEM image of CuNWs/NH_2-rGO; **d** CuNWs/NH_2-rGO/epoxy composite

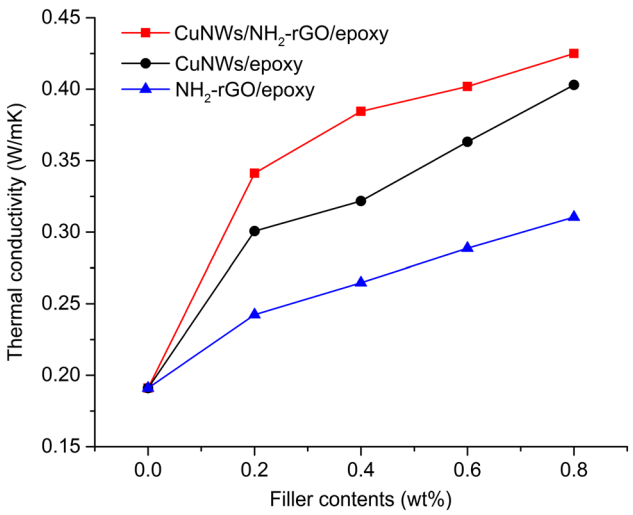

Fig. 6 Thermal conductivity of pure epoxy and its composites filled with 0.2, 0.4, 0.6, 0.8 wt% of CuNWs, NH_2-rGO, CuNWs/NH_2-rGO

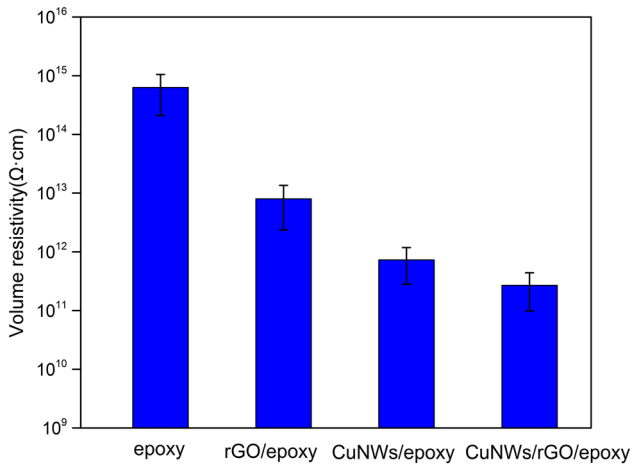

Fig. 7 Volume resistivity of pure epoxy and its composites incorporated with filler content of 0.8 wt%

which led to the high electrical conductivity of the composites. Thus, the volume conductivity of composites will decrease.

The dielectric constants of epoxy and its composites incorporated with filler content of 0.8 wt% under the frequency band from 10 to 60 MHz were shown in Fig. 8. From the curve, we can see that the dielectric constant was almost independent with the frequency in the measured frequency range from 10 to 60 MHz and the dielectric constants of the epoxy composites were all higher than the pure epoxy. Meanwhile, we can see the value of dielectric constant can be ranked as NH_2-rGO/epoxy > CuNWs/NH_2-rGO/epoxy > CuNWs/epoxy > epoxy. As known, the dielectric constant depended on the polarizability of hybrid directly. Hence, the reasons of the rank of dielectric constant can be explained as following. Firstly, compared with CuNWs/epoxy, CuNWs/NH_2-rGO/epoxy contained polar group –NH_2 and few unreacted –COOH which can be seen from FT-IR spectra above. It resulted in CuNWs/NH_2-rGO/epoxy > CuNWs/epoxy. Similarly, as for NH_2-rGO/epoxy, not only NH_2-rGO contained more polar group –NH_2 and few unreacted –COOH, but also excessive NH_2-rGO led to agglomeration or poor dispersion in the resin, weakening the restriction of the interfacial region on the molecular chain, which resulted in NH_2-rGO/epoxy > CuNWs/NH_2-rGO/epoxy.

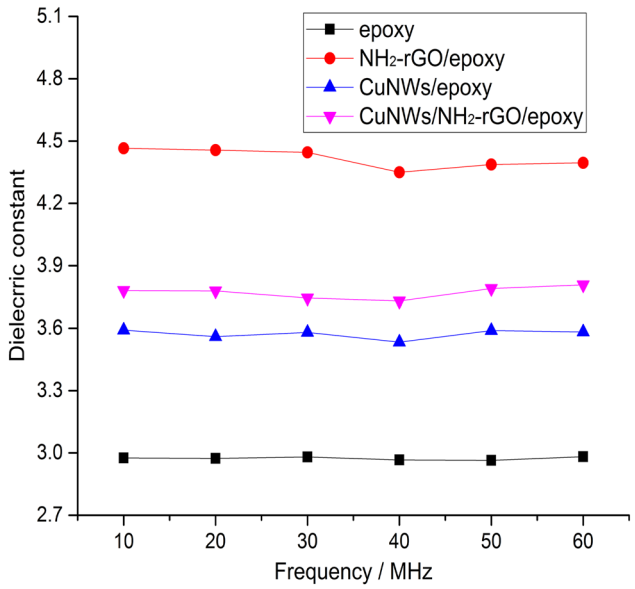

Fig. 8 Frequency dependence of dielectric constant of epoxy resin and its composites incorporated with filler content of 0.8 wt%

The thermal resistance of the composites had a major impact on the thermal property of the composites. Figure 9 showed TGA and its corresponding differential thermogravimetric (DTG) curves for pure epoxy and CuNWs/NH_2-rGO/epoxy composite incorporated with filler content of 0.8 wt% to investigate the thermal stability of composites. In the TGA curve, the char yield of CuNWs/NH_2-rGO/epoxy composite increased compared with pure epoxy. From the DTG curves we can find that the maximum degradation rate of CuNWs/NH_2-rGO/epoxy systems was lower than pure epoxy. The result confirmed that hybrid fillers can improve the thermal property of matrix. This may be attributed to the following facts. Firstly, the reaction between CuNWs/NH_2-rGO and epoxy resin contributed to a better compatibility with epoxy, which restricted the movement of polymer chain and further delayed the decomposition of polymer at high temperature. Secondly, the barrier effect of inherent characteristic layered structure of GO can work as mass-transport barrier to restrain the chain motion and substance exchange. For example, gaseous substances diffusion and the formation of new free-radicals. In addition,

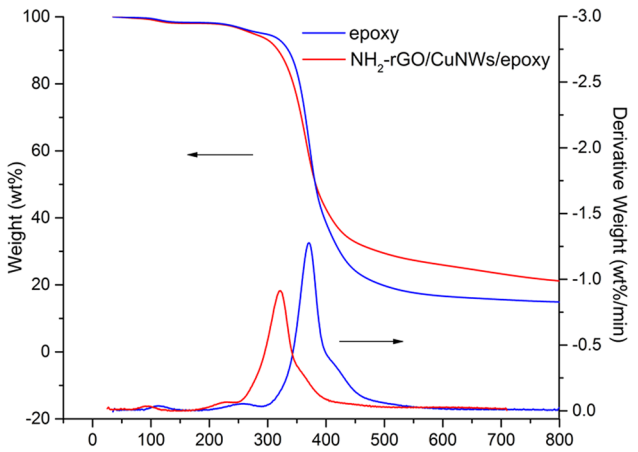

Fig. 9 TG and DTG curves of epoxy and CuNWs/NH_2-rGO/epoxy composite incorporated with filler content of 0.8 wt%

the structure characteristics of GO was similar with the carbonaceous char being formed in the process of decomposition, which can also facilitate the growth of heat insulation char layer and delayed the decomposition of composites.

4 Conclusion

CuNWs and NH_2-rGO have been successfully synthesized by a facile and effective method. Then hybrid fillers of 1-D CuNWs and 2-D reduced graphene oxide with active amino groups as additives were added into epoxy to prepare CuNWs/NH_2-rGO/epoxy composite. The result showed that the prepared CuNWs possessed high aspect ratio, uniform diameter, good dispersity and morphology. Moreover, the hybrid fillers of CuNWs and NH_2-rGO nanosheets compounded uniformly and CuNWs/NH_2-rGO/epoxy composite revealed better thermal conductivity and lower volume resistivity compared with pure epoxy and the same amount of CuNWs/epoxy and NH_2-rGO/epoxy. When the content of hybrid fillers was 0.8 wt%, the CuNWs/NH_2-rGO/epoxy composite showed the highest thermal conductivity of 0.43 W/(m · K) and lower volume resistivity of 2.69×10^{11} Ω · cm, respectively. It indicated the synergetic effect between CuNWs and NH_2-rGO. The combination of two fillers can not only improve interfacial interaction between fillers and the resin matrix but also improve thermal conductivity of composites.

References

1. Y.H. Yu, C.C.M. Ma, C.C. Teng, Y.L. Huang, H.W. Tien, S.H. Lee, I. Wang, J. Taiwan Inst. Chem. Eng. **44**, 654–659 (2013)
2. C. Pan, K. Kou, Q. Jia, Y. Zhang, G. Wu, T. Ji, Compos. Part B **111**, 83–90 (2017)
3. K. Yang, M. Gu, Compos. Part A **41**, 215–221 (2010)
4. A. Yu, P. Ramesh, M.E. Itkis, A. Elena Bekyarova, R.C. Haddon, J. Phys. Chem. C **111**, 7565–7569 (2007)
5. Y.S. Song, J.R. Youn, Carbon **43**, 1378–1385 (2005)
6. H. Tu, Y. Lin, Polym. Adv. Technol. **20**, 21–27 (2009)
7. G. Wu, Y. Cheng, Z. Wang, K. Wang, A. Feng, J. Mater. Sci. **28**, 576–581 (2017)
8. P. Ding, S. Su, N. Song, S. Tang, Y. Liu, L. Shi, Carbon **66**, 576–584 (2014)
9. G. Wu, J. Li, K. Wang, Y. Wang, C. Pan, A. Feng, J. Mater. Sci. **6544–6551**, 6544–6551 (2017)
10. C.C. Teng, C.C.M. Ma, K.C. Chiou, T.M. Lee, Compos. Part B **43**, 265–271 (2012)
11. G. Wu, Y. Cheng, K. Wang, Y. Wang, A. Feng, J. Mater. Sci. **27**, 5592–5599 (2016)
12. S. Ganguli, A.K. Roy, D.P. Anderson, Carbon **46**, 806–817 (2008)
13. Y. Xu, D. D. L. Chung, C. Mroz, Compos. Part A **32**, 1749–1757 (2001)
14. C.Y. Hsieh, S.L. Chung, J. Appl. Polym. Sci. **102**, 4734–4740 (2006)
15. L.C. Sim, S.R. Ramanan, H. Ismail, K.N. Seetharamu, T.J. Goh, Thermochim. Acta **430**, 155–165 (2005)
16. W. Zhou, S. Qi, H. Li, S. Shao, Thermochim. Acta **452**, 36–42 (2007)
17. J.M. Seuntjens, Silver and silver alloy articles, (2001)
18. T. Zhou, X. Wang, G.U. Mingyuan, X. Liu, Polymer **49**, 4666–4672 (2008)
19. H. Staleva, G.V. Hartland, Adv. Funct. Mater. **18**, 3809–3817 (2008)
20. G. Wu, H. Wu, K. Wang, C. Zheng, Y. Wang, A. Feng, RSC Adv. **6**, 58069–58076 (2016)
21. G. Wu, Y. Cheng, F. Xiang, Z. Jia, Q. Xie, G. Wu, H. Wu, Mater. Sci. Semicond. Process. **41**, 6–11 (2016)
22. A.R. Rathmell, S.M. Bergin, Y.L. Hua, Z.Y. Li, B.J. Wiley, Adv. Mater. **22**, 3558–3563 (2010)
23. R. J. Young, I. A. Kinloch, L. Gong, K.S. Novoselov, Compos. Sci. Technol. **72**, 1459–1476 (2012)
24. C. Lee, X. Wei, J.W. Kysar, J. Hone, Science **321**, 385–388 (2008)
25. M. Liu, X. Zhang, Nanoscale Res. Lett. **10**, 1–11 (2012)
26. H. Liem, H.S. Choy, Solid State Commun. **163**, 41–45 (2013)
27. A.A. Madhavan, S. Kalluri, D.K. Chacko, T.A. Arun, S. Nagarajan, K.R.V. Subramanian, A.S. Nair, S.V. Nair, A. Balakrishnan, RSC Adv. **2**, 13032–13037 (2012)
28. V. Goyal, A.A. Balandin, Appl. Phys. Lett. **100**, 073113 (2012)
29. H. Wu, L.T. Drzal, Carbon **50**, 1135–1145 (2012)
30. X. Fang, L.W. Fan, Q. Ding, X. Wang, X.L. Yao, J.F. Hou, Z.T. Yu, G.H. Cheng, Y.C. Hu, K.F. Cen, Energy Fuels **27**, 4041–4047 (2013)
31. E.H. Weber, M.L. Clingerman, J.A. King, J. Appl. Polym. Sci. **88**, 112–122 (2003)
32. G. Lee, M. Park, J. Kim, J.I. Lee, H.G. Yoon, Compos. Part A **37**, 727–734 (2006)
33. J. Chen, Y. Li, L. Huang, C. Li, G. Shi, Carbon **81**, 826–834 (2015)
34. H. Ruan, R. Wang, Y. Luo, J. Mater. Sci. **27**, 1–5 (2016)
35. A. Ghosh, D.A. Schiraldi, J. Appl. Polym. Sci. **112**, 1738–1744 (2009)
36. Y. Yu, C.M. Ma, C. Teng, Y. Huang, H. Tien, S. Lee, I. Wang, J. Taiwan Inst. Chem. Eng. **44**, 654–659 (2013)
37. S.Y. Yang, C.C.M. Ma, C.C. Teng, Y.W. Huang, S.H. Liao, Y.L. Huang, H.W. Tien, T.M. Lee, K.C. Chiou, Carbon **48**, 592–603 (2010)